ARTICLE

Hydrogenation and Ammoniation of $SrTiO_3$ for an Enhanced Visible-light Photocatalysis

Tao Sun, You-yuan Zhao, Ming Lu*

Department of Optical Science and Engineering, Key Laboratory for Micro and Nano Photonic Structures, Fudan University, Shanghai 200433, China

(Dated: Received on June 16, 2011; Accepted on December 13, 2011)

Hydrogenation and ammoniation of $SrTiO_3$ (STO), a normal ultraviolet photocatalyst, were performed by annealing STO⟨100⟩ in H_2:N_2=5%:95% and NH_3, respectively, at various temperatures T. It was found that hydrogenation at $T\geq$900 °C remarkably enhanced the UV photocatalytic ability of STO, but the visible-light photocatalysis was still unavailable, while ammoniation at $T\geq$800 °C introduced the N doping, resulting in visible-light photocatalytic activity. Furthermore, when a hydrogenated STO was subjected to ammoniation, the visible-light photocatalytic ability was nearly the same as that of the ammoniated one; but the hydrogenation of an ammoniated one significantly enhanced visible-light photocatalysis, indicating a synergetic effect of hydrogenation and ammoniation. Discussions and identifications have been made to analyze these results.

Key words: $SrTiO_3$, Hydrogenation, Ammoniation, Photocatalysis, Synergetic effect

I. INTRODUCTION

Photodecomposition of water or organic materials by semiconductors is of potential importance in sustainable energy source development and environmental protection [1, 2]. In contrast to other semiconductors, oxide semiconductors exhibit excellent photoactivity, good stability in aqueous solution, low toxicity, and low cost of production [1−4]. To match the redox potentials of water or other aqueous solutions, wide bandgap oxide semiconductors such as STO and TiO_2 have been used as photocatalysts that show photoactivity only under ultraviolet (UV)-light irradiation [1−4]. Since the UV light with <390 nm takes up only about 7% or even less of the whole solar emission energy at the ground, most of the solar emission energy becomes unavailable. Up to now, many efforts have been devoted to extending the available wavelength range for photocatalysis from UV region to visible-light one via bandgap modulation of semiconductor. Present methodologies include metal-ion doping [3, 4], non-metal-ion doping [5−10], and surface amorphism [11], aiming at narrowing the bandgap or introducing intermediate defect energy levels into the bandgap of semiconductor. On the other hand, since most of the photo-generated carriers would recombine, resulting in low photocatalytic efficiency, it is important to facilitate the motion of the carriers towards the surface and participate the redox reaction rapidly there [1−4]. Hydrogenation of TiO_2 has been found available for this purpose [12−14]. Noguchi *et al.* reported that the hydrogenated TiO_2 showed an enhanced photocatalytic performance under UV lights [12, 13]. They suggested that termination of OH groups of the defects in TiO_2 might remove recombination centers for carriers and lead to an enhanced photocatalysis. Recently, Fábrega *et al.* found that the electrochemical activity of TiO_2 nanotubes could be significantly increased after hydrogenation under UV lights [14]. It is known that ammoniation of metal oxides such as TiO_2 [5] or pervoskite oxides [15] narrows the bandgap of the oxides via substitutional N incorporations, which could cause visible-light photocatalysis.

In this work, we studied hydrogenation and ammoniation of STO⟨100⟩, we also investigated the synergetic effects of hydrogenation that improves the efficiency of photocatalysis, and ammoniation that extends the available wavelength range and makes visible-light photocatalysis possible, and eventually achieves an enhanced visible-light photocatalysis.

II. EXPERIMENTS

The starting STO samples are transparent STO⟨100⟩ from the Crystal Center of SIOM, Chinese Academy of Science. Before hydrogenation or ammoniation, the samples were supersonically cleaned in acetone and deionized water in sequence and then blown dry. For hydrogenation, the samples were annealed in the flowing forming gas of H_2:N_2=5%:95% at various temperatures (T, from 600 °C to 1000 °C) with a flow of 40 L/h, and cooled down rapidly. For ammoniation, NH_3 gas with a flow of 30 L/h was used, and T was from 600 °C to

*Author to whom correspondence should be addressed. E-mail: minglu@fudan.ac.cn

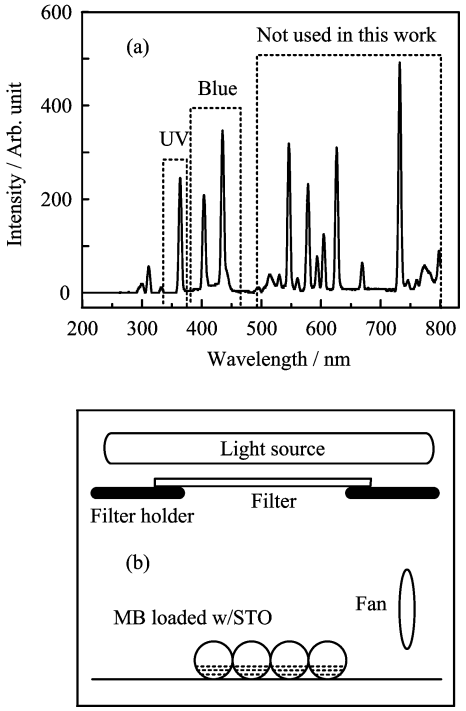

FIG. 1 Emission spectrum of the light source for experiments. The inset shows the diagram of experimental setup.

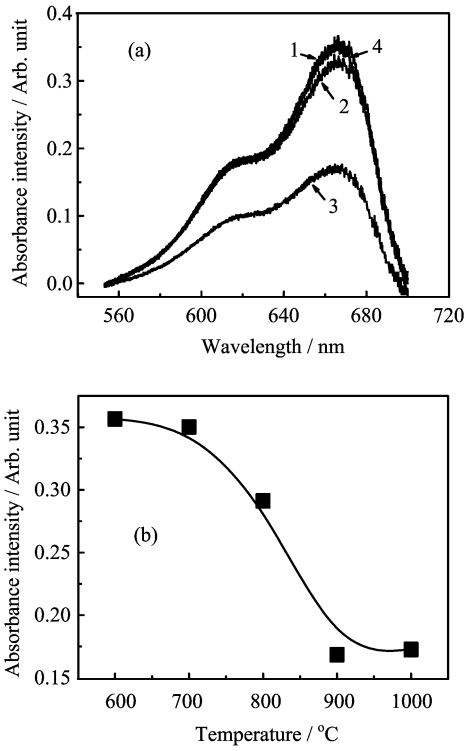

FIG. 2 (a) Absorption spectra for MB solutions. Curve 1 is for MB alone after UV irradiation, curve 2 for MB loaded with as-received STO after UV irradiation, curve 3 for MB loaded with hydrogenated STO (T=1000 °C) after UV irradiation, and curve 4 is for MB loaded with the very hydrogenated STO after blue-light irradiation. (b) The absorbance intensity of MB versus hydrogenation temperature.

1000 °C, too. The sample was cooled down naturally after annealing as did in Ref.[15]. The annealing time was 3 h for all the samples unless stated, and the light-irradiation time for photocatalysis was 20 h for all the samples. The photocatalytic activity of STO was evaluated in terms of the absorbance change of a methylene blue (MB) solution after photodecomposition by various samples. The initial concentration of MB in the solution was 0.01 mmol/L. Before light irradiation, all the samples had been placed in dark for more than 48 h. It was found that the change in MB absorbance due to the surface adsorption of various samples is negligible, and the STO-loaded MB absorption spectra were exactly the same as the pure MB (not shown here). A 400 W lamp (Heraeus, Model MDQ 401SE) served as the light source for the photocatalysis. The spectrum of the light source is shown in Fig.1. Different filters were combined so as to filter out unwanted lights and select right ones for experiments.

In this work, only the lights in UV and blue regions were used Fig.1(a). The MB would not be decomposed under irradiations of these lights without any photocatalyst. For photodecomposition of MB, each STO sample was immersed in the MB solution that was contained in the centrifugal tube in dark for 20 h, and then the MB loaded with STO was exposed to the light irradiation as illustrated in Fig.1(b). The absorption spectra were recorded at room temperature with a UV-Vis photospectrometer (WGD-8/8A, Tianjin Gangdong). Since the sample of STO⟨100⟩ has been high-temperature annealed before received, high-temperature activation is not necessary for photocatalysis experiments here. In fact, we have annealed the as-received STO at 1000 °C in air for 1 h and the absorbance of the MB loaded with such STO was found to be exactly the same as that loaded with as-received STO after UV irradiation. In order to identify the characteristics of defects, electron paramagnetic resonance (EPR) spectra were measured on Bruker ER-200D-SRC-10/12 and X-ray photoelectron spectroscopy (XPS, model Shimadzu/Kratos AXIS Ultra) was applied to examine the surface components. To assess the change in surface area, atomic force microscopy (AFM, model PSIA, XE-100) was used in non-contact mode.

III. RESULTS AND DISCUSSION

A. Hydrogenation of STO

Figure 2(a) gives four typical absorption spectra of the MB solutions after different treatments. Curve 1 stands for the MB solution alone after UV-light (λ=365 nm) irradiation. The absorption spectrum of the initial MB is the same as curve 1 (not shown here).

DOI:10.1088/1674-0068/25/01/86-90

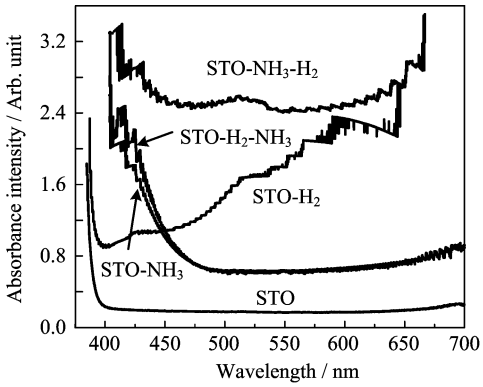

FIG. 3 Absorption spectra for the samples of STO, STO-H_2, STO-H_2-NH_3, and STO-NH_3-H_2, respectively.

Curve 2 corresponds to the MB solution loaded with as-received STO (labeled as "STO") after UV irradiation. The UV photodecomposition of MB by the STO is evidenced here. Curve 3 indicates that the hydrogenated STO at T=1000 °C (labeled "STO-H_2") can significantly enhance its UV photocatalytic activity. In Fig.2(b), the intensity of absorbance of MB, defined as the peak height at 660 nm, after UV photodecomposition by hydrogenated STO, has been plotted as a function of T for hydrogenation. However, hydrogenation of STO does not yield visible-light photocatalysis as suggested by curve 4 that represents the MB loaded with the hydrogenated STO for T=1000 °C after visible-light (λ=435 and 405 nm) irradiation.

Figure 3 gives the absorption spectra of STO and STO-H_2, respectively. It is seen that the absorption band edge is almost identical for both, suggesting that no bandgap narrowing occurs after hydrogenation. This may explain the unavailability of visible-light photocatalysis for STO-H_2. Two absorption structures are noticed for STO-H_2, peaking at λ=430 and 520 nm, respectively, and the absorption in the range of λ=390−550 nm is enhanced, which indicates the existence of defect states within the bandgap of STO due to hydrogenation. These defect states could be various oxygen-vacancy V_O defects, transition metal impurities M (M represents the residual metal ions like Fe within as-received STO) or the M-V_O complex defects which become optically activated after hydrogenation [16]. Actually, transition metal ions such as Fe and Al are common impurities in STO grown by Verneuil method, typically at a level of 10^{-5}−10^{-6} [17]. The lack of visible-light photocatalysis of the hydrogenated sample as shown in Fig.2 suggests that these defect states do not overlap effectively with the band of STO, hence the photo-generated carriers are not able to move to the surface via the valence band or conduction band of STO to fulfill the redox reaction at the surface. In fact, the non-overlap of band explains why bandgap narrowing does not occur after hydrogenation of STO.

The enhanced photocatalysis after hydrogenation

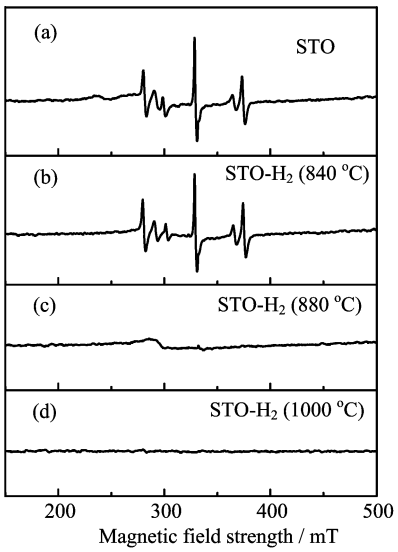

FIG. 4 EPR spectra of various STO samples at room temperature for (a) as-received STO, (b)−(d) STO hydrogenated at various temperatures.

could be due to passivation of dangling bonds intrinsically existing within STO. These dangling bonds tend to attract the photo-generated carriers and hinder their motion towards the surface. When the bonds are saturated by hydrogenation, the motion of charge carriers is promoted. Our EPR results support this suggestion. In Fig.4(a), EPR signals were observed as-received STO, indicating the existence of dangling bonds with unpaired electrons in the STO; hydrogenation made the EPR signals decrease with increasing T (Fig.4 (b)−(d)) due to hydrogen passivation of these defects. At T=1000 °C the EPR signals disappeared completely (Fig.4(d)). McCluskey *et al.* found that Sr vacancies in STO can be passivated when annealing in hydrogen at 800 °C and then cooled down rapidly [18]. van de Walle *et al.* reported similar results in ZnO [19].

Finally, it should be pointed that we have examined the surface area change after hydrogenation by AFM. It is found that the STO-H_2 is slightly rougher than the STO. After morphology measurement and surface area calculation by the attached software, the surface area of STO was found to be 1.0011 times that of the geometric surface, *i.e.* an ideally flat and plane surface, and that of STO-H_2 was just 1.0021 times that of the geometric one. However, in Fig.2(a), the absorbance of MB loaded with STO after UV irradiation is 91.0% that of pure MB, while the absorbance of MB loaded with STO-H_2 is only 42.8% that of pure MB, it is then clear that the change in surface area is a negligible factor here in enhanced photocatalysis.

B. Ammoniation of STO

In Fig.5(a), curve 1 stands for the absorbance of the MB solution alone after visible-light (λ=435 and

DOI:10.1088/1674-0068/25/01/86-90

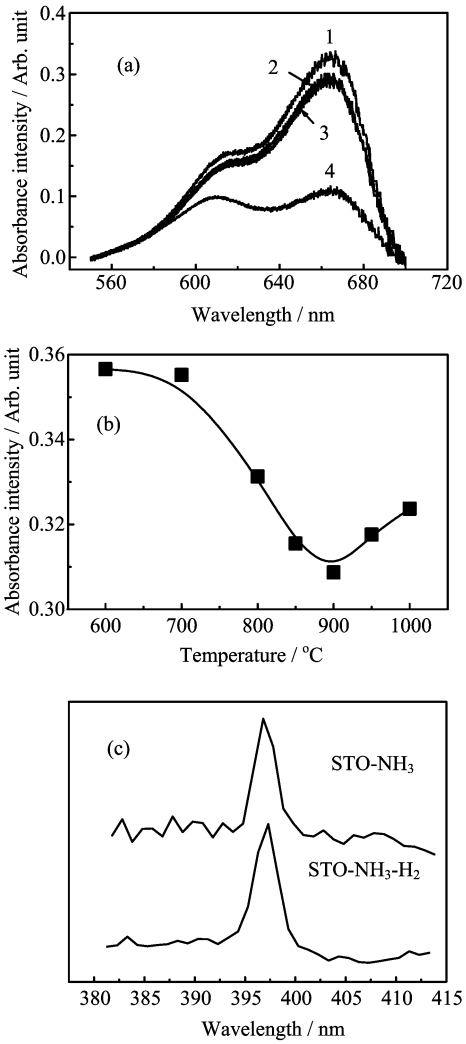

FIG. 5 (a) Absorption spectra for MB solutions. Curves 1 and 2 stand for MB alone and loaded with ammoniated STO at T=900 °C, respectively. Curves 3 and 4 are for the STO samples hydrogenated and ammoniated sequentially, and treated reversly, respectively. (b) The absorbance intensity of MB at λ=660 nm versus ammoniation temperature. All the samples have been blue-light irradiated. (c) The N1s signals of XPS for STO-NH_3 and STO-NH_3-H_2, respectively.

405 nm) irradiation. The absorption spectrum of the initial MB is the same as curve 1 (not shown here), indicating that these visible lights did not decompose the MB. Curve 2 corresponds to the MB solution loaded with the ammoniated STO at 900 °C (labeled as STO-NH_3) after visible-light irradiation. Visible-light photocatalysis occurs in contrast to the case of hydrogenation. This is because ammoniation could incorporate nitrogen into the STO and the N2p derived states overlap strongly with the maximum of the valence band of the STO, making the bandgap narrowing [5, 15]. This has actually been reflected in Fig.3, where the absorption band edge of STO-NH_3 shifts from 390 nm of the UV region to about 460 nm of the blue-light one with respect to that of STO. In Fig.5(b), the intensity of absorbance of MB after visible-light photodecomposition by ammoniated STO versus anneal temperature T of STO has been plotted. It is seen that ammoniation at T=900 °C of STO is most effective for visible-light photocatalysis. Figure 5(c) gives the N1s signal (about 397 eV) of XPS from STO-NH_3. The N1s signal has been adjusted by C1s. The signal located at about 397 eV has been ascribed to substitutional N ions [5, 20]. The EPR result shows that after ammoniation even at T=900 °C (Fig.6(a)), the main structures of EPR signal remain, indicating that no passivation occurs during ammoniation.

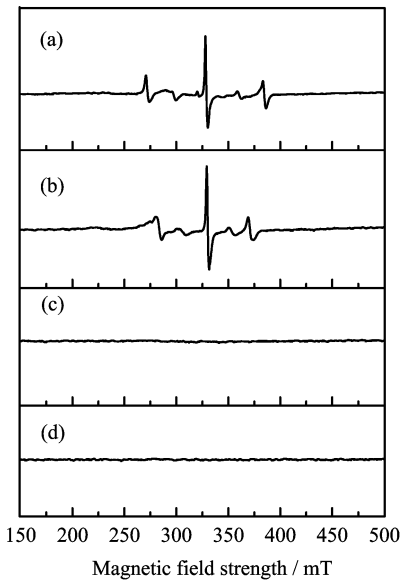

FIG. 6 EPR spectra of various STO samples. (a) STO-NH_3, (b) STO-H_2-NH_3, (c) STO-H_2, and (d) STO-NH_3-H_2.

C. Synergetic effect of hydrogenation and ammoniation of STO

We now explore the synergetic effects of hydrogenation and ammoniation. As shown by curve 3 in Fig.5(a), which corresponds to the case of STO hydrogenated and then ammoniated (labeled as STO-H_2-NH_3), the visible-light photocatalytic activity of STO-H_2-NH_3 was close to that of STO-NH_3. This is because the hydrogen passivation effect would fade away during ammoniation, as similar to the case of Si nanocrystal thin films, where high temperature annealing in nitrogen would expel the incorporated hydrogen and make the passivation ineffective [21]. The EPR results of Fig.6 (b) and (c) support this conclusion. It is seen that in the STO-H_2-NH_3 (Fig.6(b)), the EPR signal recovered as compared to the STO-H_2 (Fig.6(c)). Therefore the procedure of successive hydrogenation and ammoniation is unable to realize nitrogen doping together with

DOI:10.1088/1674-0068/25/01/86-90

hydrogen passivation, and no synergetic effect exists. In Fig.3 the absorption spectrum of STO-H_2-NH_3 has been given, which resembles that of STO-NH_3.

Then we examine the case of ammoniation and then hydrogenation. The visible-light photocatalysis is now significantly enhanced as indicated by curve 4 in Fig.5(a). In Fig.5(c), N1s signal in STO-NH_3-H_2 is also shown. This synergetic effect reveals that for the sample of STO-NH_3-H_2, both nitrogen incorporation due to ammoniation and passivation from hydrogenation are realized. The EPR results of Fig.6 (c) and (d) suggest that hydrogen passivation has been achieved in the STO-NH_3-H_2 sample, as the EPR signal of STO-NH_3-H_2 (Fig.6(d)) disappears as in the sample of STO-H_2 (Fig.6(c)). On the other hand, nitrogen incorporation still remains as reflected in Fig.5(c). In Fig.3 the absorption spectrum of STO-NH_3-H_2 was also presented. Bandgap narrowing is observed as compared to STO-H_2, and meanwhile the absorption in the range of λ=390−550 nm is much enhanced as compared to both STO-NH_3 and STO-H_2-NH_3. Therefore, for the sample of STO-NH_3-H_2, the doped nitrogen is to narrow the bandgap of STO, extend the utilizable photons and make the visible-light photocatalysis available; meanwhile, hydrogen passivation improves the efficiency of photogenerated charge carriers. The combination of both shows a synergetic effect that significantly promotes the visible-light photocatalysis.

IV. CONCLUSION

Hydrogenation of STO can result in passivation of defects in the STO, which could enhance the photocatalysis via facilitating the motion of photo-generated carrier towards the surface to participate the redox reaction there, but the bandgap remains unchanged. Ammoniation of STO, on the other hand, can dopes N ions, which narrows the bandgap of STO and makes visible-light photocatalysis available. It has been found that successive hydrogenation and ammoniation of STO produces a visible-light photocatalytic activity close to that of the ammoniated one; however, the reverse anneal of STO can achieve N-doping and passivation together, and significantly enhance the visible-light photocatalysis. The synergetic effect suggests that proper combination of different treatments of STO might make a strong and visible-light photocatalysis possible.

V. ACKNOWLEDGMENTS

This work was supported by the National Natural Science Foundation of China (No.10974034 and No.60638010). We thank Pei-nan Wang and Lan Mi for their assistance in experiments.

[1] A. Fujishima and K. Honda, Nature **238**, 37 (1972).
[2] M. R. Hoffmann, S. T. Martin, W. Choi, and D. W. Bahnemann, Chem. Rev. **95**, 69 (1995).
[3] W. Choi, A. Termin, and M. R. Hoffmann, J. Phys. Chem. **98**, 13669 (1994).
[4] W. Choi, A. Termin, and M. R. Hoffmann, Angew. Chem. **106**, 1148 (1994).
[5] R. Asahi, T. Morikawa, T. Ohwaki, K. Aoki, and Y. Taga, Science **293**, 269 (2001).
[6] S. U. M. Khan, M. Al-Shahry, and W. B. Ingler Jr., Science **297**, 2243 (2002).
[7] X. Chen and C. Burda, J. Am. Chem. Soc. **130**, 5018 (2008).
[8] H. Irie, Y. Watanabe, and K. Hashimoto, J. Phys. Chem. B **107**, 5483 (2003).
[9] J. C. Yu, J. Yu, W. Ho, Z. Jiang, and L. Zhang, Chem. Mater. **14**, 3808 (2002).
[10] T. Umebayashi, T. Yamaki, H. Itoh, and K. Asai, Appl. Phys. Lett. **81**, 454 (2002)
[11] X. Chen, L. Liu, P. Y. Yu, and S. S. Mao, Science **331**, 746 (2011).
[12] D. Noguchi, Y. Kawamata, and T. Nagatomo, Jpn. J. Appl. Phys. **42**, 5255 (2003).
[13] D. Noguchi, Y. Kawamata, and T. Nagatomoa, J. Electrochem. Soc. **151**, D61 (2004).
[14] C. Fàbrega, T. Andreu, F. Güell, J. D. Prades, S. Estradé, J. M. Rebled, F. Peiró, and J. R. Morante, Nanotechnology **22**, 235403 (2011).
[15] R. Aguiar, A. Kalytta, A. Reller, A. Weidenkaff, and S. G. Ebbinghaus, J. Mater. Chem. **18**, 4260 (2008).
[16] B. Jalan, R. Engel-Herbert, T. E. Mates, and S. Stemmer, Appl. Phys. Lett. **93**, 052907 (2008).
[17] A. Frye, *Ph. D. Dissertation*, Philadelphia: University of Pennsylvania, No.9953529, (1999).
[18] M. C. Tarun and M. D. McCluskey, J. Appl. Phys. **109**, 063706 (2011).
[19] E. V. Lavrov, J. Weber, F. Borrnert, C. G. van de Walle, and R. Helbig, Phys. Rev. B **66**, 165205 (2002).
[20] X. Chen and C. Burda, J. Phys. Chem. B **108**, 15446 (2004).
[21] Z. Q. Xie, D. Chen, Z. H. Li, Y. Y. Zhao, and M. Lu, Nanotechnology **18**, 115716 (2007).

DOI:10.1088/1674-0068/25/01/86-90